1975

The Production of 45Ca from the Isotopes of Titanium at 350 MeV

Dennis Paul Swauger
College of William & Mary - Arts & Sciences

THE PRODUCTION OF ^{45}Ca FROM THE ISOTOPES OF TITANIUM AT 350 MeV

A Thesis

Presented to

The Faculty of the Department of Chemistry

The College of William and Mary in Virginia

In Partial Fulfillment

Of the Requirements for the Degree

Master of Arts

---

by

Dennis Paul Swauger

May 1975

APPROVAL SHEET

This thesis is submitted in partial fulfillment of

the requirements for the degree of

Master of Arts

Dennis Paul Swauger

Dennis Paul Swauger

Approved, May 1975

Richard L. Kiefer

Richard L. Kiefer

S. Young Tyree, Jr

S. Young Tyree

Eric Herbst

Eric Herbst

ACKNOWLEDGMENTS

The writer wishes to express his sincere appreciation and thanks to all of his family, friends, and professors, who made this work possible through their encouragement and guidance throughout this investigation. Notable among these are Dr. Richard L. Kiefer for his suggestion of the project and his guidance throughout, Drs. S. Young Tyree, Jr., and Eric Herbst for their careful reading of the manuscript, the writer's parents for their endless encouragement, Drs. David W. Thompson, Robert A. Orwoll, and Randolph A Coleman for their encouragement and instruction, and Mr. Edward Katz for his patience and helpful discussions.

The writer is also grateful to the College of William and Mary for a teaching assistantship and fellowship, and to the Space Radiation Effects Laboratory and the physics department of the College of William and Mary for the use of their facilities.

TABLE OF CONTENTS

LIST OF TABLES

LIST OF FIGURES

ABSTRACT

Cross sections for the production of ^{45}Ca from ^{47}Ti, ^{48}Ti, ^{49}Ti, and ^{50}Ti were experimentally measured using 350 MeV protons. This work was performed in order to determine if the direct knockout of ^{4}He clusters contributes significantly to the intermediate energy reaction cross sections of these medium weight nuclei. The cross sections show a significant increase at the ^{49}Ti and ^{50}Ti isotopes, showing that the reactions (p, p^{4}He) and (p, p^{4}He n) are probably contributing to the measured cross sections.

THE PRODUCTION OF ^{45}Ca FROM THE ISOTOPES OF TITANIUM AT 350 MeV

I. INTRODUCTION

A nuclear reaction is a process in which a nucleus reacts with another nucleus, an elementary particle, or a photon to produce one or more other nuclei and possibly other particles (4). Most of the nuclear reactions studied have been induced by light particles (neutrons, protons, deuterons, tritons, helium ions, electrons, mesons, photons) (4). Most of the published work has been done using protons as incident particles. In this work, protons have been used as the incident particles, also.

Proton-induced reactions can be characterized according to the energy of the incident protons. Below approximately 50 MeV, these reactions can be thought of as occurring through the formation of a compound nucleus in which the proton is captured by the target nucleus and its energy is randomly distributed among the nucleons of the nucleus (4). The nucleus then de-excites by the evaporation of particles (or the emission of a photon) in a process similar to the evaporation of molecules from a drop of liquid (4).

The energy region between 50- and 100-MeV has not been studied as extensively as the other energy regions, but it seems evident that compound nucleus formation becomes less important and other processes (that is, direct interactions) become more important.

The other processes previously mentioned become evident in

the energy region above 100 MeV where most reactions take place by direct interaction between the incident protons and the nucleons of the target nuclei. Above 400 MeV, direct interaction is still the most important process, but pion processes become increasingly more important. Pions are the particles that are thought to be exchanged between nucleons in a nucleus to give the strong, short-range nuclear force. The threshold for the production of pions with protons is 280 MeV. At this energy and above, pions (either π^+, π^-, or π^o, depending on the type of collision) can be produced in the bombardment. Although the threshold for pion production is 280 MeV, they are not produced significantly below 400 MeV.

Intermediate energy (>100 MeV) proton-induced reactions can be explained in the framework of the cascade-evaporation model. This is the commonly accepted model for intermediate energy nuclear reactions, and consists of two stages (4):

1. A knock-on cascade in which the incident particle interacts with a single nucleon in the struck nucleus. These collision partners may then pass through the nucleus without further interaction, or one or both may make further collisions. Thus, a nucleonic cascade is developed, the exact nature of which depends upon the probability for and the kinematics of each collision (12). At the end of the cascade, the nucleus is left in an excited state, the excitation energy arising from the equilibration of the kinetic energy of those cascade particles which remain in the

nucleus, and the "particle hole" energy which results from the ejection of bound nucleons (12). The ejection of a bound nucleon leaves a vacancy in one of the energy states within the nuclear potential well; the resulting excitation energy caused by the vacancy is the "particle hole" energy.

2. The excited cascade products may then de-excite in at least two ways:

a. By the evaporation of nucleons or clusters of nucleons, in a way similar to the evaporation of particles from compound nuclei.

b. By dividing into two roughly equal pieces in a process analogous to fission.

The assumption in the cascade stage that the incident proton interacts with only a single nucleon at a time is based on the "impulse approximation" (11). This approximation is based on the following assumptions:

1. For high energy protons, the energy of the proton is much larger than the interaction energy between nucleons in the nucleus, and its wavelength is less than the average distance between nucleons (4).

2. Any interaction between the incident proton and any of the nucleons is nearly the same as if both particles were in free space, rather than inside a nucleus (4).

On the basis of the "impulse approximation," protons of a few hundred MeV have a mean free path in nuclear matter of about

3×10^{-13} cm, which is of the same order as nuclear radii.

It has been shown in recent years that in reactions induced by intermediate- and high-energy protons, heavier particles (D, He, Li, Be, B nuclei) are emitted from the target nuclei (12). These heavier particles may be evaporated from the nucleus, or, since some have considerable kinetic energy and are emitted at small angles, they may be directly ejected from the nucleus. Clusters of nucleons are thought to have a transient existence in the low-density, diffuse edge of nuclei, since the average distance between nucleons in this region is large compared to the range of the nucleon-nucleon force (4). Collisions between nucleons in this low density region could form clusters if the internucleon forces were strong enough, since collisions involving any momentum transfers are forbidden by the Pauli principle because all states of lower momentum are already occupied (4). ^{4}He clusters are especially thought to exist in nuclei since ^{4}He is a very stable entity.

This study was undertaken to determine, through the measurement of the production cross section of ^{45}Ca from the separated stable isotopes of titanium, if a direct reaction of the type (p, p^{4}He) is possible in these nuclei. Assuming that such reactions are possible, the reactions of interest are

$$^{47}\text{Ti(p, 3p)}^{45}\text{Ca}$$

$$^{48}\text{Ti(p, 3pn)}^{45}\text{Ca}$$

$^{49}Ti(p, p^{4}He)^{45}Ca$

$^{50}Ti(p, p^{4}Hen)^{45}Ca$

A substantial increase in cross section at the 49 and 50 isotopes should give preliminary evidence for such reactions.

As stated earlier, most intermediate- and high-energy proton-induced reactions can be explained in the framework of the cascade evaporation model. Since all the reactions in this work were run at 350 MeV, this model should still be a valid framework, since inclusion of the direct interaction with heavier particles would simply add to the existing model.

II. EXPERIMENTAL

Target Preparation

The isotopes used in the irradiations were ^{47}Ti, ^{48}Ti, ^{49}Ti, and ^{50}Ti. All were available in enriched form from Oak Ridge National Laboratory, although each of the enriched isotopes was contaminated by all of the other stable titanium isotopes. The largest contaminant in all of the enriched isotopes was ^{48}Ti, since it has the largest natural abundance of the isotopes. The percentage of ^{48}Ti in ^{47}Ti, ^{49}Ti, and ^{50}Ti isotopes was 16.5, 18.54, and 17.8 respectively. Contamination by the other isotopes amounted to between 1% and 2% in all the samples except ^{48}Ti, which was 99.13% enriched. Corrections were made to the cross sections for all contamination. Isotopic and spectrographic analysis of all the enriched isotopes are shown in Table 1.

Targets were prepared by depositing a layer of enriched TiO_2 on a tared 2" x 2" piece of 1 mil aluminum foil. This was accomplished by slurrying approximately 10 mg of enriched TiO_2 with dry ethyl ether and pouring the mixture onto the foil, using a Millipore filter and chimney apparatus. After allowing the ether to evaporate, there remained a thin, uniform layer of TiO_2 on the foil. The average area of the deposit was 10.3 cm^2. The foil and

TABLE 1

Target Materials

Target nuclide	Natural abundance (%)	Form bombarded	Isotopic analysis		Spectrographic analysis	
			Isotope	Atomic percent	Element	Percent
^{47}Ti	7.28	TiO_2	46	1.9	Ag	.01
			47	79.5	Al	.05
			48	16.5	B	.01
			49	1.1	Ba	.01
			50	1.0	Be	.001
					Bi	.02
					Ca	.01
					Cb	.05
					Cd	.05
					Co	.05
					Cr	.05
					Cs	.05
					Cu	.01
					Fe	.02
					Ge	.05

TABLE 1 (Continued)

Target nuclide	Natural abundance (%)	Form bombarded	Isotopic analysis		Spectrographic analysis	
			Isotope	Atomic percent	Element	Percent
					Hg	< .05
					K	< .01
					Li	< .005
					Mg	< .01
					Mn	< .02
					Mo	< .02
					Na	< .01
					Ni	< .05
					Pb	< .02
					Pt	< .05
					Rb	< .02
					Sb	< .05
					Si	.03
					Sr	< .01
					Sn	< .02
					Ta	< .05
					V	< .02

TABLE 1 (Continued)

Target nuclide	Natural abundance (%)	Form bombarded	Isotopic analysis		Spectrographic analysis	
			Isotope	Atomic percent	Element	Percent
					W	< .05
					Zn	< .2
					Zr	< .05
^{48}Ti	73.94	TiO_2	46	0.25	Ag	< .02
			47	0.26	Al	< .05
			48	99.13	B	.01
			49	0.19	Ba	< .02
			50	0.17	Ca	< .02
					Cb	< .05
					Cd	< .05
					Co	< .05
					Cr	< .02
					Cu	< .02
					Fe	< .01
					K	< .01
					Li	< .005

TABLE 1 (Continued)

Target nuclide	Natural abundance (%)	Form bombarded	Isotopic analysis		Spectrographic analysis	
			Isotope	Atomic percent	Element	Percent
					Mg	< .01
					Mn	< .01
					Mo	< .02
					Na	< .01
					Ni	< .05
					Pb	< .05
					Pt	< .02
					Rb	< .02
					Si	.03
					Sn	< .02
					Sr	< .01
					Ta	< .05
					V	< .02
					W	< .05
					Zr	< .05

TABLE 1 (Continued)

Target nuclide	Natural abundance (%)	Form bombarded	Isotopic analysis		Spectrographic analysis	
			Isotope	Atomic percent	Element	Percent
^{49}Ti	5.51	TiO_2	46	1.58	Al	.05
			47	1.58	B	.01
			48	18.54	Ba	.01
			49	76.14	Be	.001
			50	2.16	Bi	.02
					Ca	.01
					Cb	.05
					Cd	.05
					Co	.05
					Cr	.05
					Cs	.05
					Cu	.01
					Fe	.02
					Ge	.05
					K	.01
					Li	.005
					Mg	.01

TABLE 1 (Continued)

Target nuclide	Natural abundance (%)	Form bombarded	Isotopic analysis		Spectrographic analysis	
			Isotope	Atomic percent	Element	Percent
					Mn	< .02
					Mo	< .02
					Na	< .01
					Ni	< .05
					Pb	< .02
					Pt	< .05
					Rb	< .02
					Sb	< .05
					Si	.03
					Sn	< .02
					Sr	< .01
					Ta	< .05
					V	< .02
					W	< .1
					Zn	< .2
					Zr	< .05

TABLE 1 (Continued)

Target nuclide	Natural abundance (%)	Form bombarded	Isotopic analysis		Spectrographic analysis	
			Isotope	Atomic percent	Element	Percent
^{50}Ti	5.34	TiO_2	46	2.0	Ag	< .01
			47	1.8	Al	< .05
			48	17.8	B	< .01
			49	2.0	Ba	< .01
			50	76.4	Be	< .001
					Bi	< .02
					Ca	< .01
					Cb	< .05
					Cd	< .05
					Co	< .05
					Cr	.05
					Cs	< .05
					Cu	< .01
					Fe	.07
					Ge	< .05
					Hg	< .05

TABLE 1 (Continued)

Target nuclide	Natural abundance (%)	Form bombarded	Isotopic analysis		Spectrographic analysis	
			Isotope	Atomic percent	Element	Percent
					K	< .01
					Li	< .005
					Mg	< .01
					Mn	< .02
					Mo	< .02
					Na	< .01
					Ni	< .05
					Pb	< .02
					Pt	< .05
					Rb	< .02
					Sb	< .05
					Si	.01
					Sn	< .02
					Sr	< .01
					Ta	< .05
					V	< .02

TABLE 1 (Continued)

Target nuclide	Natural abundance (%)	Form bombarded	Isotopic analysis		Spectrographic analysis	
			Isotope	Atomic percent	Element	Percent
					W	< .05
					Zn	< .2
					Zr	< .05

deposit were then weighed and the thickness of the deposit was calculated in mg/cm^2.

The TiO_2 deposits were coated with a thin film of Duco cement in order to prevent flaking of it during handling and irradiation. The foil and deposit was then cut as shown in Figure 1.

Target packets for the irradiations were made up as shown in Figure 2. All of the target packets contained either three or four of the titanium isotopes, with ^{48}Ti in all of them. The guard foils were 3/4" x 1" pieces of 1 mil aluminum foil. Monitor foils of 99.99+% purity and 1.5 mil were placed at each end of the target packet in order to moniter the proton beam. They were placed both at the front and back, so as to show any attenuation of the beam through the target or to show if secondary particles were contributing to the induced activities, although the contribution of secondaries should have been made negligible by the use of thin targets. Cover foils were wrapped about the other foils to hold them together during irradiation.

Irradiations

All irradiations were carried out on the 600 MeV synchrocyclotron at the Space Radiation Effects Laboratory (SREL) in Newport News, Virginia. The targets to be irradiated were placed in a holder as shown in Figure 3 and were mounted on the probe head. Since the energy of the protons used in the irradiations is dependent

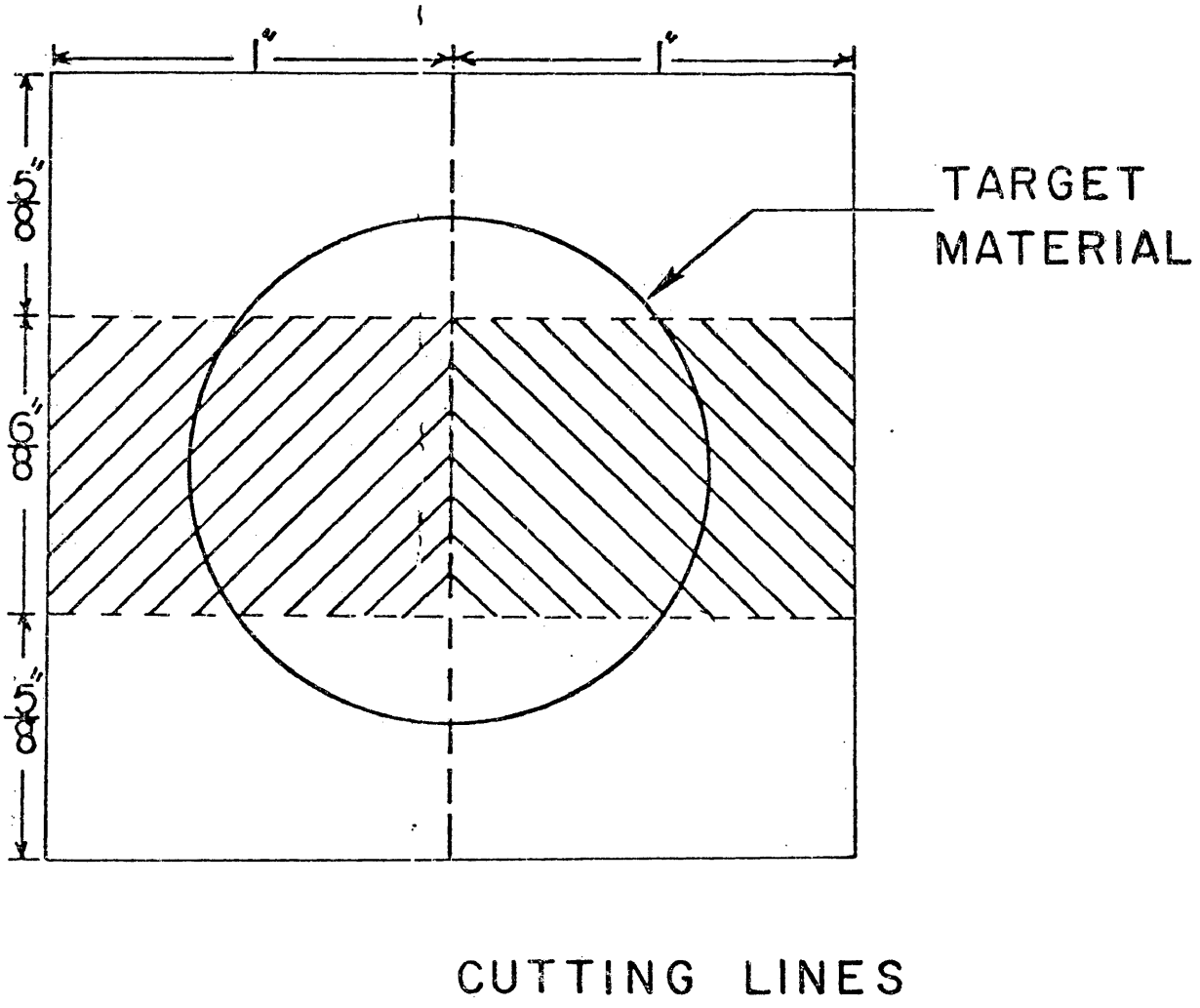

Fig. 1. Detail of taget foil.

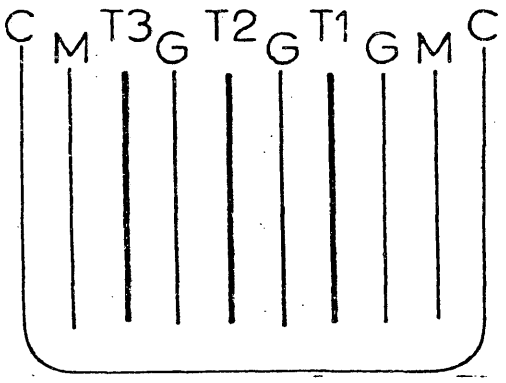

C COVER FOIL
M MONITOR FOIL
G GUARD FOIL
T1 FIRST TARGET FOIL(^{47}Ti, ^{48}Ti, ^{49}Ti, or ^{50}Ti)
T2 SECOND TARGET FOIL(^{47}Ti, ^{48}Ti, ^{49}Ti, or ^{50}Ti)
T3 THIRD TARGET FOIL(^{47}Ti, ^{48}Ti, ^{49}Ti, or ^{50}Ti)

Fig. 2. Schematic diagram of irradiation packet.

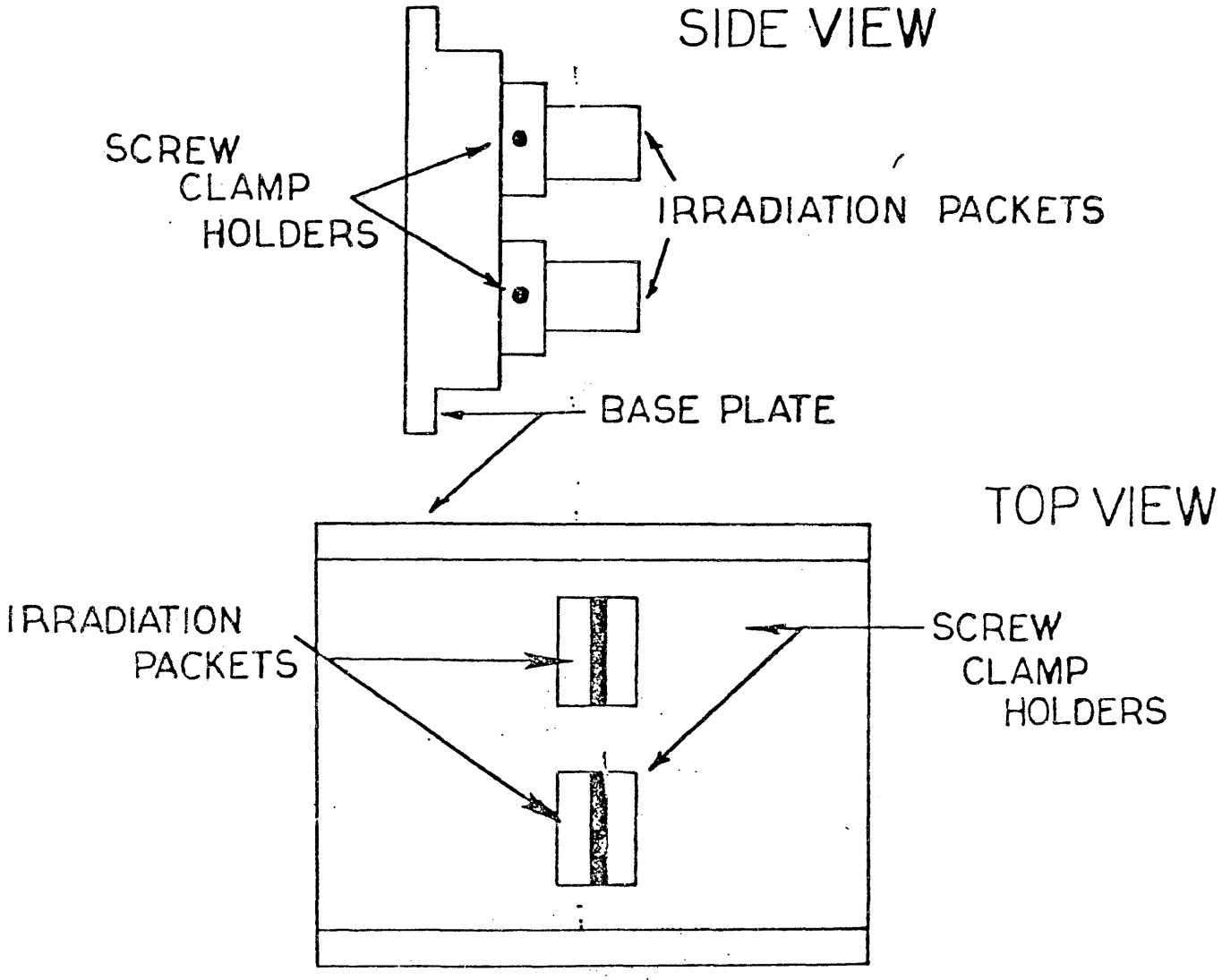

Fig. 3. Target holder assembly.

on the radial distance of the targets from the center of the cyclotron, appropriate settings were made for 350 MeV protons. All targets were irradiated for 30 minutes with the full available beam intensity. The proton beam was monitored with the reaction $^{27}Al(p, 3p3n)^{22}Na$ (1).

Chemistry

The intensity of the proton beam passing through the target falls off sharply with the distance from the leading edge of the target, as shown in Figure 4 (10). Therefore, any misalignment of the targets would result in different targets being exposed to different numbers of protons. To minimize any effects of misalignment, a 1/2" x 1/2" section of each target was punched 1/8" from the leading edge, using the apparatus shown in Figure 5.

Using the 1/2" x 1/2" punched section, the cover foils were discarded and the monitors were set aside to be mounted on aluminum counting cards. Calcium was then separated from the target foils and their corresponding guard foils by a method adapted from Kolthoff and Sandell (6, 7).

Each aluminum target foil (with TiO_2) and its corresponding guard foil were dissolved in hot, concentrated HCl. After the careful addition of 5 ml of a saturated Na_2SO_4-H_2SO_4 solution, the mixture was heated to boiling and allowed to cool; 10 ml of a carrier solution of 0.506 mg/ml Ca^{2+} was then added.

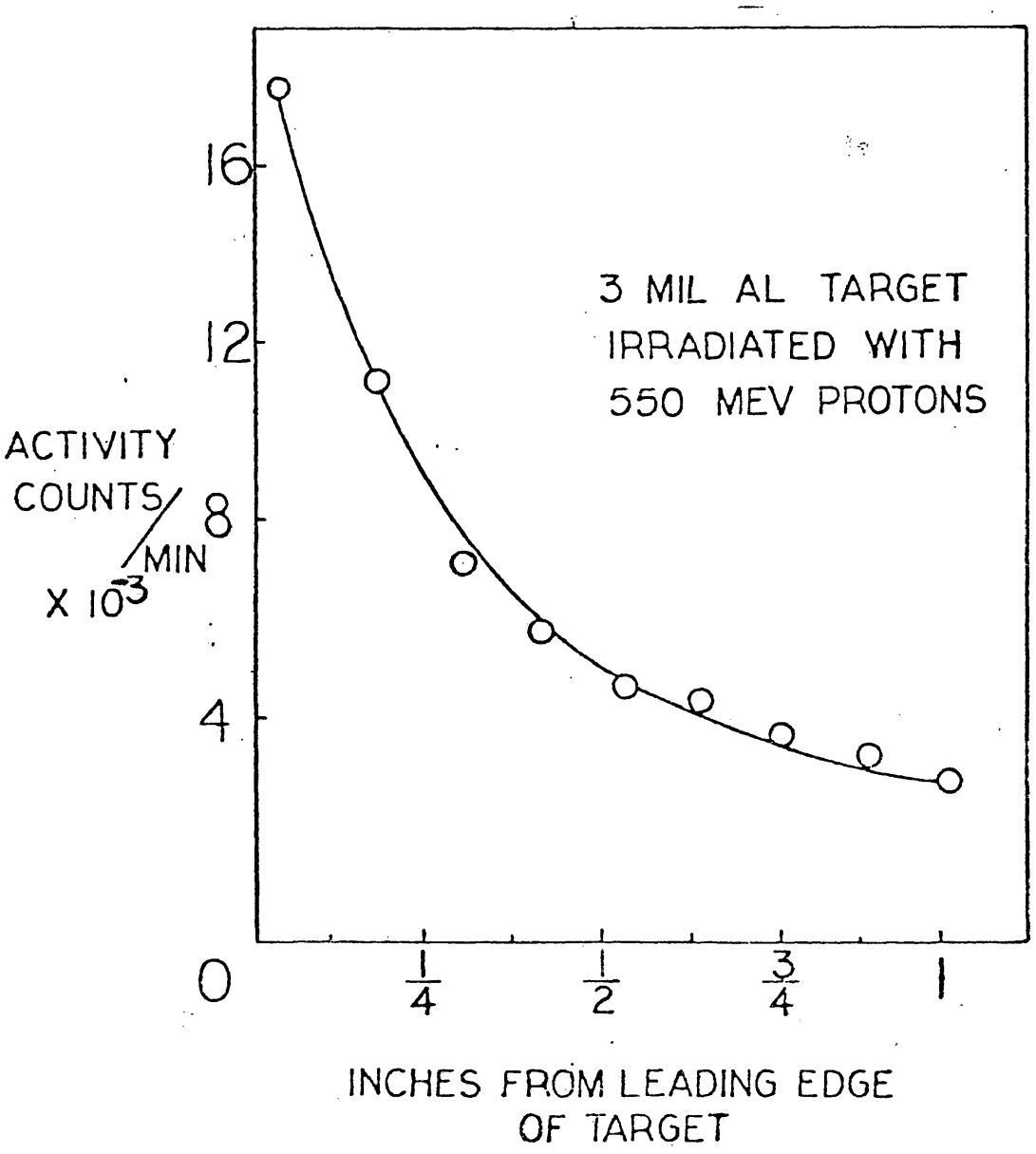

Fig. 4. Induced acitivity in target versus distance from leading edge of target.

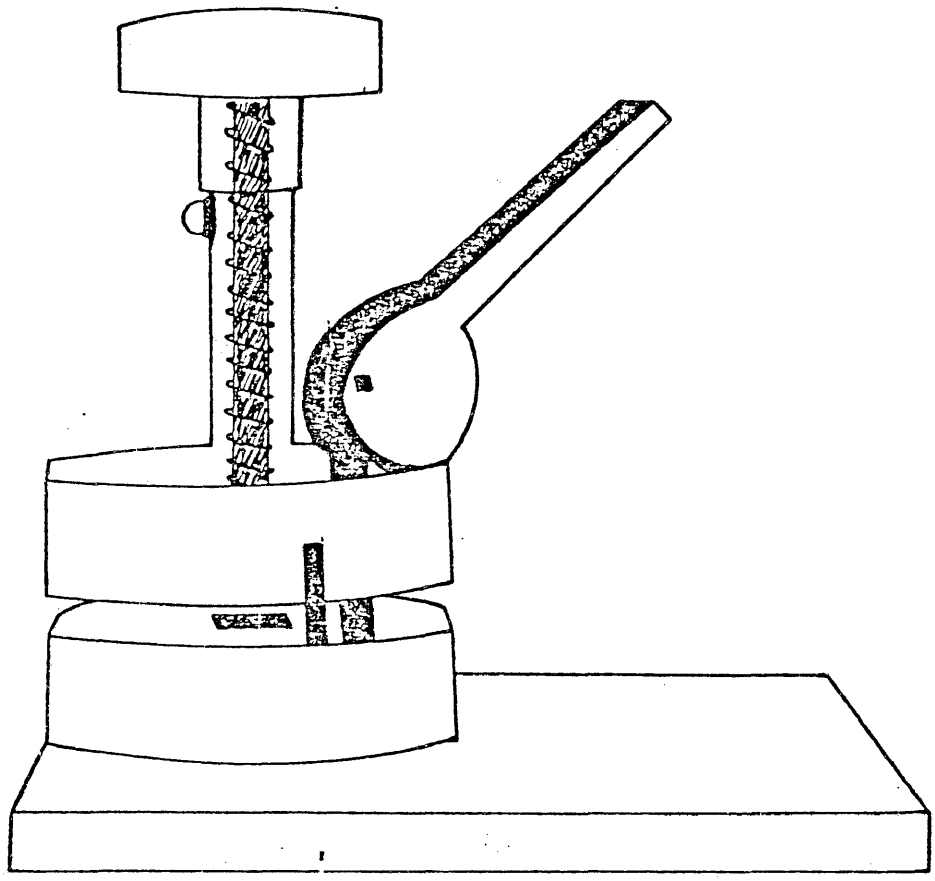

Fig. 5. Punch for cutting irradiated samples.

Using methyl red, the pH of the solution was adjusted to ~4 using concentrated NH_4OH. This quantitatively precipitated the titanium as a hydrated oxide complex and aluminum as the hydroxide. The solution was filtered with a glass fiber filter, leaving a clear, yellow solution. To the filtrate was added 10 ml of a saturated $Na_2C_2O_4$ solution, and heating the mixture precipitated the calcium as calcium oxalate. The solution was allowed to stand undisturbed for a few hours, and the precipitate was filtered on Whatman #42 filter paper and washed with 0.1% $Na_2C_2O_4$.

The precipitate was then redissolved in 20 ml of hot 1:4 HCl, and the filter paper was washed with 1:100 HCl. Methyl red was added, and the solution was diluted to 80 ml with distilled water. Then 5 ml of the saturated $Na_2C_2O_4$ solution was added and 1:1 NH_4OH was added until the red color of the solution changed to yellow. The solution was allowed to sit overnight, quantitatively precipitating the calcium oxalate, which was collected on a tared piece of Whatman #42 filter paper, and was dried at 100°C for approximately six hours.

The filter paper containing the calcium precipitates was then weighed, and mounted on aluminum counting cards, covered with 0.25 mil Mylar film for counting of the ^{45}Ca activity.

Measurement of Radioactivity

The decay scheme of ^{45}Ca is shown in Figure 6. The 165-day half life and 100% β^- decay of this nuclide made the separation and counting of the samples very convenient.

The ^{45}Ca samples were counted using a methane flow proportional counter of the type shown in Figure 7, surrounded by lead shielding to limit background radiation. High voltage must be applied to the counter wire loop, and this was supplied by a Fluke high voltage power supply. Pulses were amplified with a Canberra Industries preamplifier and double delay line amplifier. Unwanted pulses were rejected with a Canberra Industries discriminator. Pulses passing through the discriminator were counted using a Hamner scaler, and counting times were recorded using a Hamner timer/scaler. A diagram of the basic circuit used for the beta counting is shown in Figure 8.

After all amplifier and discriminator settings were made, the counting rate of a standard source was determined as a function of high voltage settings. A "plateau" was reached where the counting rate was independent of the high voltage value. An appropriate high voltage setting (3,300 volts) along the plateau was used for all the beta counting.

The counter cannot detect all of the radiation from the samples because of the small solid angle subtended by the counter,

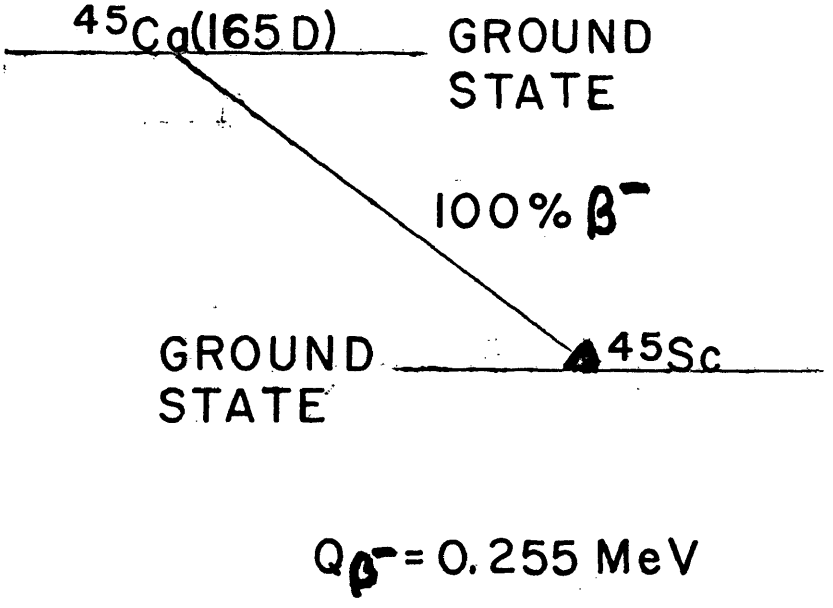

Fig. 6. Decay scheme of calcium -45.

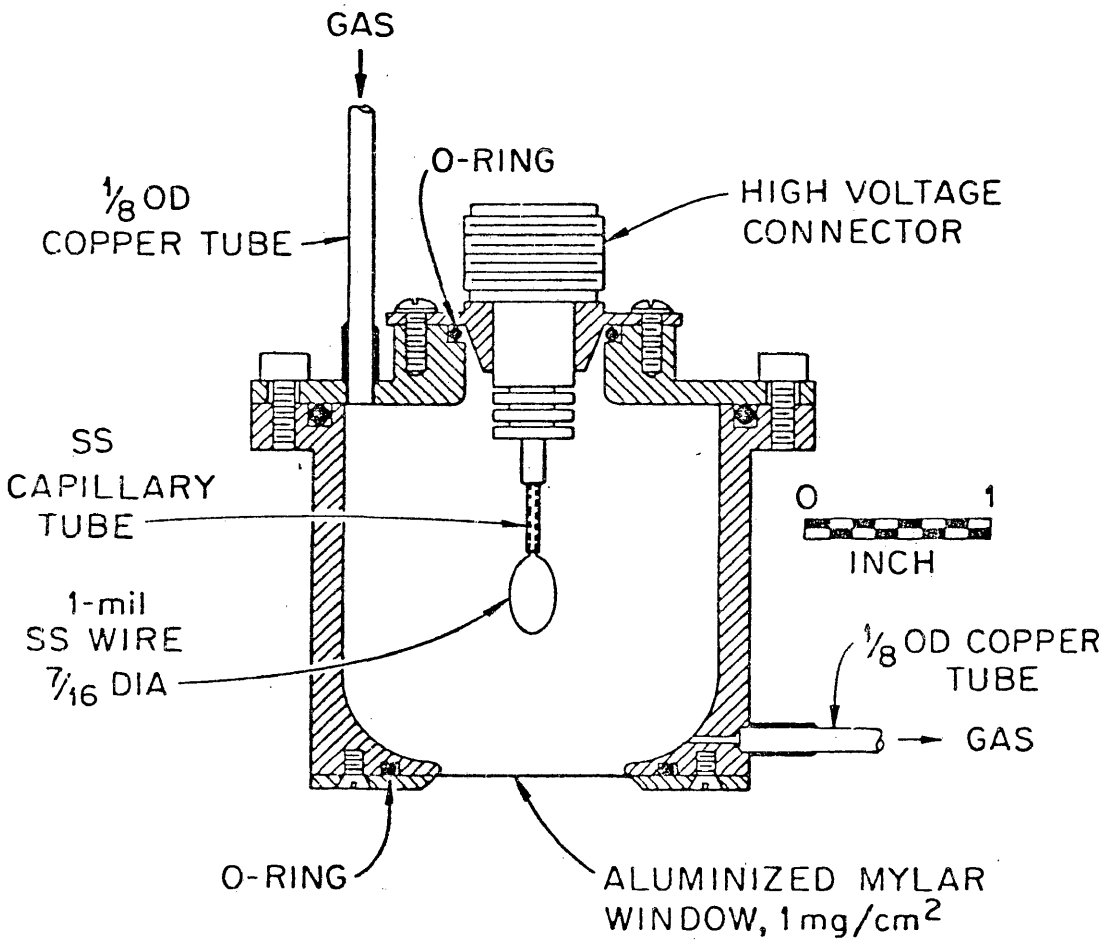

Fig. 7. Gas flow proportional counter from reference 14.

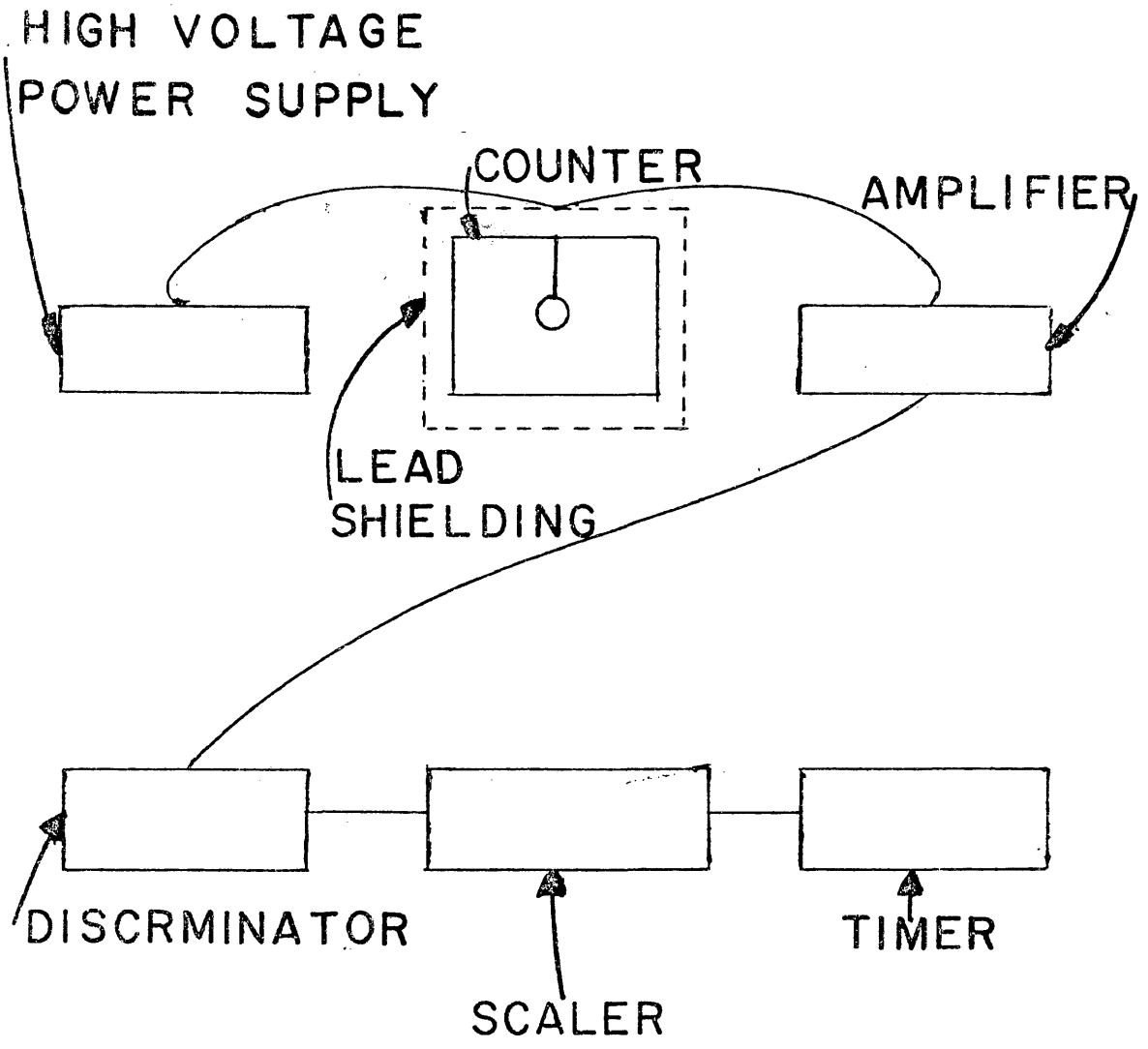

Fig. 8. Schematic diagram of beta counting apparatus.

self-absorption of β^- particles in the samples, absorption of β^- particles in the mylar covering the samples or in the end window of the counter, et cetera. Absolute disintegration rates were determined by the use of samples of ^{45}Ca of known disintegration rates (9). A standard solution of ^{45}Ca was obtained from New England Nuclear Corporation containing 2.73 microcuries per milliliter of ^{45}Ca. Different thicknesses of calcium oxalate precipitates were made, each containing the same amount of ^{45}Ca. These were counted, and the detection efficiency of the counter was determined as a function of sample thickness, as shown in Figure 9. The detection efficiency of the counter for the samples from the irradiations could then be determined, since the thickness of each sample was known.

Quantitative measurements of the activity of the monitors were made by counting the 1.274 MeV gamma ray of ^{22}Na. The arrangement used for counting the monitor activities is shown in Figure 10.

The detector used was a Harshaw integral line unit including a 3" x 3" sodium iodide crystal (activated with thallium) and a photomultiplier tube. The magnitude of the output pulse from the detector is proportional to the energy of the detected radiation. These pulses were amplified and stored in a Victoreen PIP 400-channel pulse height analyzer, where pulses are stored according to their energy. Data was recorded with a Teletype page printer. High voltage

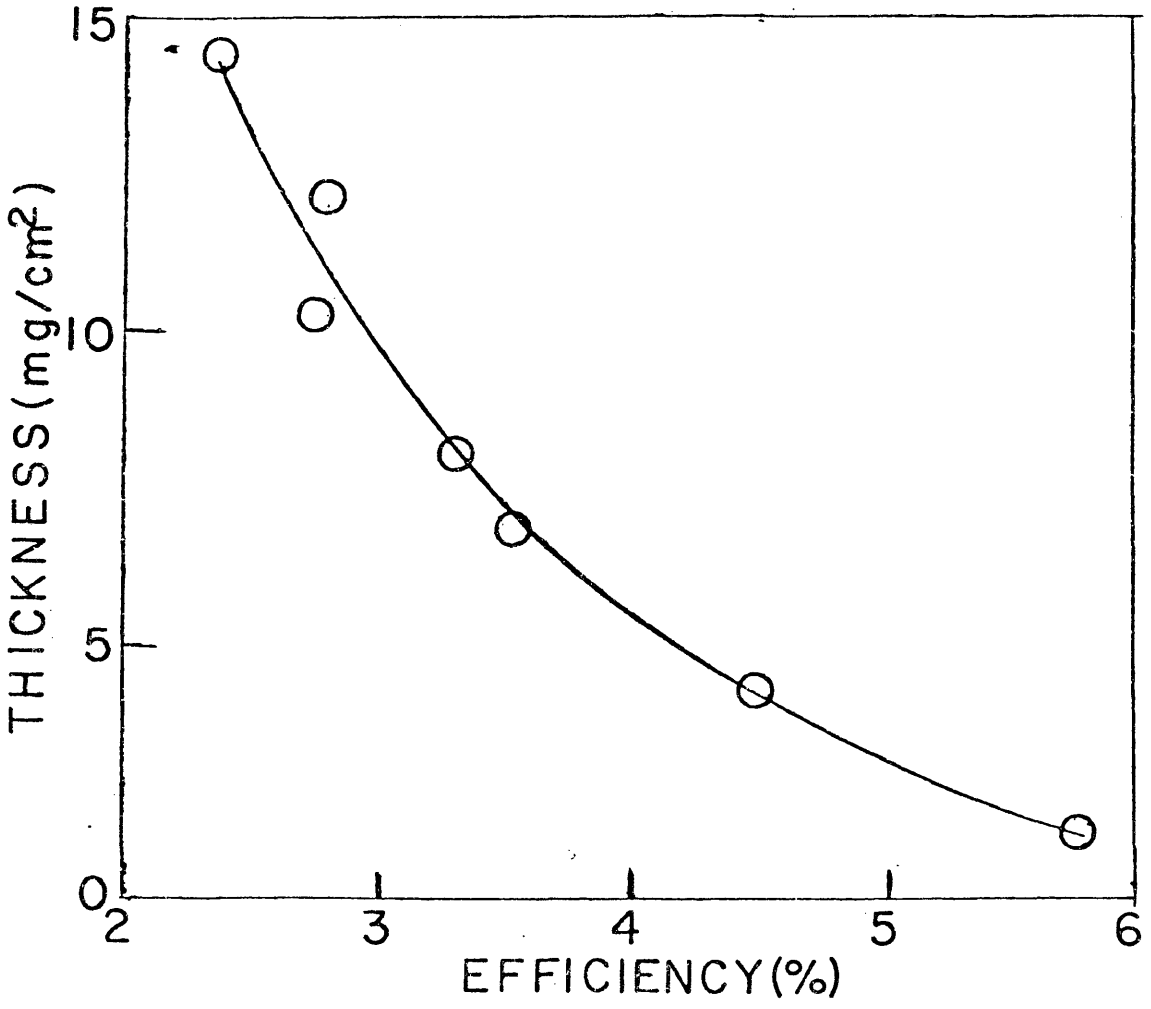

Fig. 9. Thickness of standard samples versus counter efficiency.

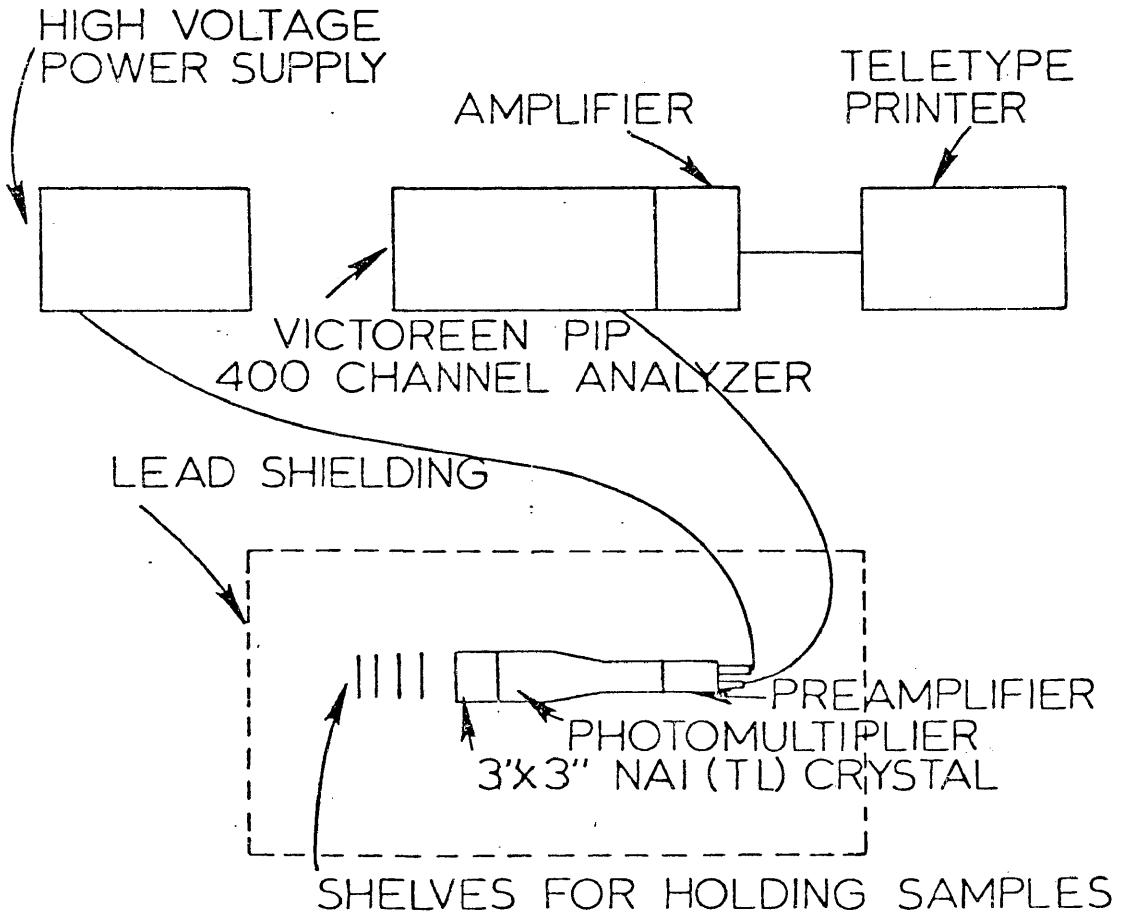

Fig. 10. Schematic diagram of Gamma counting apparatus.

was provided to the photomultiplier tube by a Fluke high voltage DC power supply. Background radiation was minimized by surrounding the detector with lead shielding.

Absolute disintegration rates of the monitors were determined by calibrating the counting arrangement with a standard ^{22}Na source obtained from the National Bureau of Standards.

Chemical Yields

Chemical yields of Ca^{2+} in both the samples separated from the irradiated targets and the standard samples used in the calibration were determined by titration of the samples with EDTA (3). This method was used instead of the weights of the samples, since, by weight, all chemical yields were greater than 100%. This was believed to be due to $Na_2C_2O_4$ and to the variation in the number of waters of hydration of the calcium oxalate compound.

The precipitates were dissolved in 20 ml of 2N H_2SO_4 and neutralized with 2N NaOH. Then, 5 ml of a magnesium-EDTA solution was added to the solution in order to make the end point sharper. The solution was then buffered to pH 10, diluted to 50 ml, and titrated with 9.94×10^{-3} M EDTA at $60^{\circ}C$, using Eriochrome black T as the indicator. The visual end point was reached when the color of the solution changed from red to blue. One milliliter of the EDTA solution was equivalent to 0.398 mg Ca^{2+}.

Calculations

The activity of a given radioactive species at time t = 0 is related to the activity at any given later time by the relationship

$$A_o = \frac{A}{e^{-\lambda t}} \tag{1}$$

where A_o is the activity at t = 0, A is the activity at time t, and λ is the decay constant of the species under investigation. The half life ($t_{1/2}$) of a given radioactive species is the time required for the activity of a sample to fall to one-half of its original value and is equal to $\ln 2/\lambda$ (4). Taking the logarithm of both sides of equation (1) yields

$$\ln A = \ln A_o - \lambda t \tag{2}$$

Plotting ln A versus time gives a straight line with slope $-\lambda$ and intercept $\ln A_o$.

The ^{45}Ca samples were counted six times within a period of at least six weeks. Background counts were taken each day and were subtracted from the observed counting rates of the samples, all counting rates being normalized to counts per minute.

Since all of the activity of the samples could be attributed to the 165-day ^{45}Ca isotope, the initial activities of the samples were calculated by a computer program based on the least-squares method of analysis. The activities versus time were fed into the

program and these points were fit to a line of slope $-\lambda$, where λ is given by $\ln 2/t_{1/2}$. Figure 11 shows a typical plot obtained.

The area enclosed by the 1.274 MeV photopeak of ^{22}Na is a measure of the activity due to this isotope. A computer program was used to fit a Gaussian curve to the observed photopeak, to integrate the area under the curve, and to subtract off an exponential background count from the total area under the Gaussian. The activities at the end of the irradiations were then calculated using equation (1).

The number of atoms of a radioactive species at the end of an irradiation is given by

$$N_o = \frac{A_o}{(ce)(cy)\ \lambda(1-e^{-\lambda t})} \qquad (3)$$

where N_o is the number of atoms produced, A_o is the initial activity of the sample, ce is the detection efficiency of the counter, cy is the chemical yield of the sample, and $1-e^{-\lambda t}$ is a factor to correct N_o for the decay of the species during irradiation (12). For short irradiations and long-lived nuclides, the relationship reduces to

$$N_o = \frac{A_o}{(ce)(cy)\lambda} \qquad (4)$$

The cross section of a nuclear reaction is a measure of the probability for that reaction taking place. Cross sections are usually expressed in units of the barn (b, 10^{-24} cm^2) or the millibarn (mb, 10^{-27} cm^2).

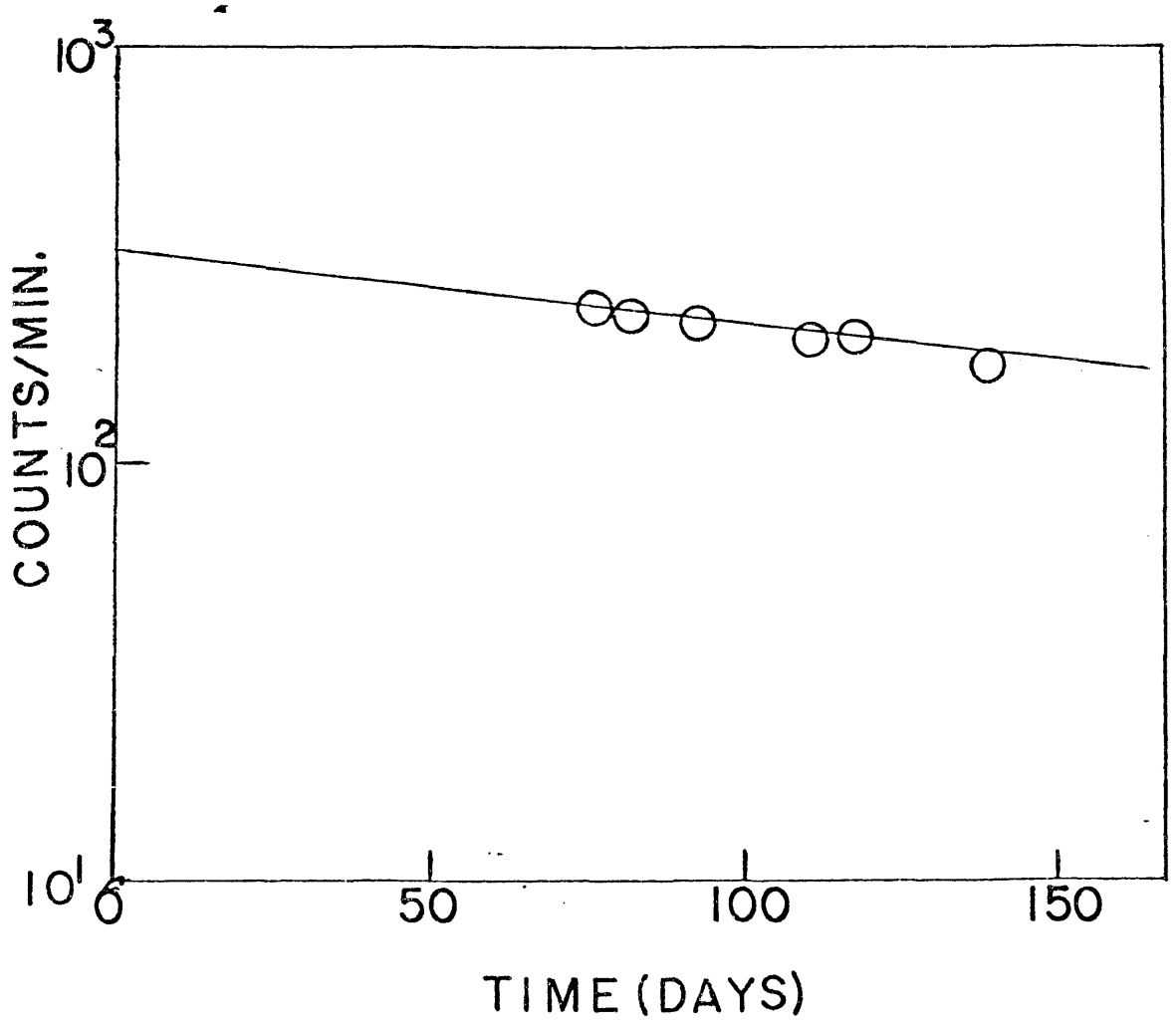

Fig. 11. Typical plot of ^{45}Ca decay.

When a beam of particles is negligibly attenuated in passing through a target, the cross section, σ, for a particular process is

$$\sigma = \frac{N_o}{pt} \tag{5}$$

where N_o is calculated from equation (4), p is the number of incident particles which passed through the target, and t is the thickness of the target in atoms/cm^2 (12). The monitors were used to determine the number of protons which passed through the targets, since values of the cross sections for the reaction $^{27}Al(p, 3p3n)^{22}Na$ at different energies were available. The number of incident protons is then

$$p = \frac{N_o(^{22}Na)}{\sigma m \; t_m} \tag{6}$$

where σm is the value of the cross section for the monitor reaction at the energy used in the irradiations, and t_m is the thickness of the monitor foil in atoms/cm^2. Combination of equations (5) and (6) gives

$$\sigma s = \sigma m \frac{N_o(^{45}Ca)}{N_o(^{22}Na)} \frac{t_m}{t_s} \tag{7}$$

where σs is the production cross section for ^{45}Ca and t_s is the thickness of the target in atoms/cm^2 (12).

The calculated cross sections were finally corrected for contamination by ^{48}Ti, where any contribution from this isotope was

subtracted from the ^{47}Ti, ^{49}Ti, or ^{50}Ti cross section.

III. RESULTS

The production cross sections for ^{45}Ca from the titanium isotopes are given in Table 2. Uncertainty in the value of the monitor cross section is reported to be $\pm$ 10% (1). The energy spread of the protons within the cyclotron is estimated to be between $\pm$ 3- to $\pm$ 4-% (5). The uncertainty in the chemical yields due to errors in reading the burettes is $\pm$ 1%. Counting efficiency errors due to uncertainties in chemical yields and activities of standard samples amout to $\pm$ 2%. Uncertainties in the ^{45}Ca activities are $\pm$ 4- to $\pm$ 5-% due to fitting the activity versus time data to a line of slope $-\lambda$. Errors in the gamma counting efficiencies and activities are $\pm$ 1- to $\pm$ 2-% in both cases. An error of $\pm$ 5% was estimated for nonuniformities of the TiO_2 deposit on the target foil. The total uncertainty, which was calculated as the square root of the sum of the squares of the pertinent errors (4), was calculated to be $\pm$ 13%.

TABLE 2

Cross Sections for the Production of ^{45}Ca from ^{47}Ti, ^{48}Ti, ^{49}Ti, and ^{50}Ti in Millibarns (10^{-27} cm^2)

Individual runs	Individual runs
^{47}Ti	^{48}Ti
1.94	4.10
2.33	4.03
1.84	4.75
1.65	3.74
1.76	4.06
Mean value = 1.90 ± 0.25	Mean value = 4.14 ± 0.54
^{49}Ti	^{50}Ti
8.16	9.26
7.06	9.76
10.30	10.90
10.50	8.19
8.44	9.46

TABLE 2 (Continued)

Individual runs	Individual runs
7.71	Mean value = 9.51 $\pm$ 1.24
Mean value = 8.69 $\pm$ 1.13	

IV. DISCUSSION

The values of the cross sections in Table 2 are consistent with other cross sections for similar reactions at this energy and in this region of the periodic chart. As can be seen, the cross section values for the ^{49}Ti and ^{50}Ti isotopes increase substantially over those for ^{47}Ti and ^{48}Ti.

Dubost, et al. (2) studied the recoil of ^{4}He from gold, bismuth, and thorium targets with 157 MeV protons. They found a substantial contribution (about 40 mb $\pm$ 10 for all the targets) to the total ^{4}He cross sections that could be attributed to the knockout of these clusters. Lefort, et al. (8) went even further and measured the contribution of direct interaction processes to the total cross sections for ^{3}H and ^{3}He in addition to ^{4}He from gold, bismuth, and thorium. The contributions they measured amounted to 40 mb $\pm$ 3 for ^{4}He, 4 mb $\pm$ 0.5 for ^{3}He, and 21 mb $\pm$ 3.5 for ^{3}H. The term "direct interaction" includes not only knockout of preformed clusters by incident protons, but also includes pickup mechanisms within the nucleus, where prompt cascade nucleons pick up one or two other nucleons before leaving the nucleus, stripping mechanisms where ^{4}He loses a neutron or a proton before leaving the nucleus, and the knockout of clusters by cascade neutrons, protons, or other clusters within the nucleus.

The contribution from evaporation to the observed total cross sections for ^{4}He, ^{3}He, and ^{3}H in this work was, in most cases, greater than or equal to the direct interaction cross sections. This shows that the cascade evaporation model is a valid framework, but it needs to include interactions with clusters during the cascade stage, since it is now evident that this stage is much more complex than was originally proposed.

As can be seen in the work of Dubost and Lefort, ^{4}He clusters have the greatest probability of emission of the clusters considered in both the direct interaction and evaporation cases. This is probably because of the great stability of ^{4}He as compared to ^{3}H or ^{3}He. ^{4}He has a binding energy of approximately 7 MeV/nucleon, as compared to about 2.5 MeV/nucleon in the cases of ^{3}H and ^{3}He.

In the light of the work of Dubost (2) and Lefort (8), it would be reasonable to expect an increase in ^{45}Ca cross section with an increase in the atomic weight of the titanium isotopes. The cross section at the ^{47}Ti isotope can be explained only in terms of the (p, 3p) reaction, which does not include any contributions from the direct interaction with or the evaporation of clusters of nucleons. The cross section for ^{45}Ca from ^{48}Ti could have some contribution from the (p, $p^{3}He$) reaction, which may account for its slightly higher cross section. There are numerous reaction paths through which ^{45}Ca

can be produced from ^{49}Ti and ^{50}Ti. These include many possible reactions in which there could be direct interaction with clusters of nucleons, including those such as (p, p^{4}He) and (p, p^{4}He n). Since there are so many reaction paths that the two heaviest of the isotopes could take, including either the knockout or evaporation of the highly stable ^{4}He nucleus, it would seem logical that the probability of these reactions would increase.

An investigation of the kind presented in this paper, where the cross section of one nuclide was measured from four consecutive isotopes of the same atomic number, was never performed before. It would seem that studies of this type could give rather good information about the different reaction mechanisms that contribute to cross sections in intermediate and high energy proton-induced reactions. Also, there is a definite lack of experimentally determined cross sections of products from individual isotopes in this mass region and at these intermediate energies.

Even though this work did not say anything about the kinetic energy or angles of emitted clusters or nuclides, it does show some kind of definite structure in the reaction mechanisms that these titanium isotopes follow to produce ^{45}Ca. It would be of considerable interest to perform a radiochemical recoil study of both the angles and energies of ^{45}Ca recoils and/or clusters emitted from these reactions. A study of the variation of the ^{45}Ca cross sections from

the individual isotopes with varying energy (maybe from 100- to 400-MeV) would also be of interest in order to determine if the cross sections measured here for ^{49}Ti and ^{50}Ti are simply a function of the energy, or if there are definitely effects caused by the existence of clusters.

There was about 1% difference in the activity of the front and rear monitors of all the targets. This shows that secondary particles were not formed to any appreciable extent during the irradiation.

V. RESULTS OF MONTE CARLO CALCULATIONS

Monte Carlo cascade calculations taken from Chen, et al. (13), were run using the four titanium isotopes and 350 MeV protons. The STEPNO version of Vegas, as the computer program is called, was used, since it generally gives the best correlation with the experimentally determined cross sections. This particular version of the calculation uses a step function to approximate the nuclear density distribution and divides the nucleus into seven concentric regions, each of constant density (13). It also assumes that there is no refraction or reflection of cascade nucleons when they cross from one region into another (13).

Although this program does not include any interaction with clusters during the cascade, it can show the probability for and excitation energy of nuclides from a simple cascade mechanism. Table 3 shows the results of the calculations for those cascade products that could give ^{45}Ca after the evaporation step. For each isotope, one thousand cascades were calculated.

As can be seen in the table, the most probable reactions at this energy are (p, p), (p, 2p), (p, pn), (p, 2pn), and (p, p2n). Considering these reactions and their relatively low average excitation energies, it would seem unlikely that much ^{45}Ca would be produced from ^{49}Ti and ^{50}Ti after evaporation, since this would involve the evaporation of several nucleons in each case. From the

TABLE 3

Results of Cascade Calculations

Reaction	Cross section (mb)	Average excitation energy
	^{47}Ti	
(p, p)	11.00	28.39
(p, 2p)	12.30	19.70
(p, 3p)	4.84	65.23
	^{48}Ti	
(p, p)	7.81	40.11
(p, 2p)	14.3	26.52
(p, 3p)	1.34	56.69
(p, pn)	20.70	38.97
(p, 2pn)	10.90	65.40
(p, 3pn)	2.45	83.98
(p, n)	4.68	46.10

TABLE 3 (Continued)

Reaction	Cross section (mb)	Average excitation energy
	^{49}Ti	
(p, p)	11.30	47.71
(p, 2p)	11.10	42.84
(p, 3p)	2.03	87.10
(p, pn)	24.20	33.69
(p, 2pn)	10.20	60.42
(p, 3pn)	1.81	74.39
(p, p2n)	7.23	78.51
(p, 2p2n)	4.75	98.56
(p, 3p2n)	1.81	88.61
(p, n)	4.07	57.84
(p, 2n)	2.71	58.56
	^{50}Ti	
(p, p)	12.80	53.67
(p, 2p)	15.30	32.56

TABLE 3 (Continued)

Reaction	Cross section (mb)	Average excitation energy
(p, 3p)	1.60	87.62
(p, pn)	21.30	38.43
(p, 2pn)	7.10	65.45
(p, 3pn)	2.06	68.73
(p, p2n)	8.93	82.50
(p, 2p2n)	4.81	106.65
(p, 3p2n)	1.83	73.62
(p, p3n)	0.69	91.53
(p, 2p3n)	2.29	83.71
(p, 3p3n)	0.46	121.47
(p, n)	5.72	45.62
(p, 2n)	3.89	113.38
(p, 3n)	1.60	124.33

reactions and average excitation energies of the cascade products of ^{47}Ti and ^{48}Ti, it would seem likely that the calculated ^{45}Ca cross sections from these nuclides would be comparable to those from ^{49}Ti and ^{50}Ti. Experimentally this was not found, thus lending support to the effects caused by the inclusion of clusters during the cascade step.

A stepwise outline of the basic steps in the calculation is given in Appendix C.

Bibliography

Bibliography

(1) J. B. Cummings, Ann. Rev. Nucl. Sci. 13, 261(1963).

(2) H. Dubost, M. Lefort, J. Peter, and X. Tarrago, Phys. Rev. 136, B1618(1964).

(3) H. A. Flaschka, EDTA Titrations, New York, Pergamon Press (1964).

(4) Gerhart Friedlander, Joseph W. Kennedy, and Julian Malcolm Miller, Nuclear and Radiochemistry, New York, John Wiley and Sons (1964).

(5) David Hopp (Virginia Associated Research Center), private communication.

(6) I. M. Kolthoff, and Philip J. Elving, Treatise on Analytical Chemistry, Part II, Vol. 4, New York, Interscience Publishers (1966).

(7) I. M. Kolthoff, and E. B. Sandell, Textbook of Quantitative Inorganic Analysis, New York, Macmillan (1952).

(8) M. Lefort, J. P. Cohen, H. Dubost, and X. Tarrago, Phys. Rev. 139, B1500(1965).

(9) B. P. Bayhurst, and R. J. Preswood, Nucleonics 17, 82(1959).

(10) Thomas J. Ruth, A Comparison of (p, 2n) and (p, pn) Reaction on Cerium-140 at Intermediate Energies, College of William and Mary (1967).

(11) R. Serber, Phys. Rev. 72, 1114(1947).

(12) L. Yaffe, ed., Nuclear Chemistry, Vol. I, New York, Academic Press, (1968).

(13) K. Chen, Z. Fraenkel, G. Friedlander, J. R. Grover, J. M. Miller, and Y. Shimamoto, Phys. Rev. 166, 949(1968).

Appendix

APPENDIX A

SAMPLE CALCULATION: ^{49}Ti,

DETERMINATION 1

Target Preparation

weight target + Al 0.1903 g

weight Al 0.1841 g

weight target 0.0062 g

$$\text{area} = 9.84 \text{ cm}^2$$

$$\text{thickness} = \frac{6.20 \text{ mg}}{9.84 \text{ cm}^2}$$

$$= 0.630 \text{ mg/cm}^2$$

$$\text{MW } TiO_2(^{49}Ti \text{ enriched}) = (.0158)(45.952) + (.0158)(46.952) + (.1854)(47.948) + (.7614)(48.948) + (.0216)(49.945)$$

$$= 80.74 \text{ g/mole}$$

$$\text{1/2" x 1/2" punched target} = (1.27 \text{ cm})^2$$

$$= 1.61 \text{ cm}^2$$

in 1.61 cm^2 punched target,

$$\text{mg } TiO_2 = (0.630 \text{ mg/cm}^2)(1.61 \text{ cm}^2)$$

$$= 1.01 \text{ mg } TiO_2$$

mg Ti(^{49}Ti enriched) in 1/2" x 1/2" target $= \frac{(1.01 \text{ mg } TiO_2)(48.74 \text{ mg Ti/m mole})}{(80.74 \text{ mg } TiO_2/\text{m mole})}$

$= 0.610$ mg Ti

Chemistry

5.06 mg Ca carrier added to each sample

weight ppt. + filter paper	0.0881 g
weight filter paper	0.0688 g
weight ppt.	0.0193 g

$\text{area} = 2.43 \text{ cm}^2$

$\text{thickness} = \frac{19.3 \text{ mg}}{2.43 \text{ cm}^2}$

$= 7.94 \text{ mg/cm}^2$

$Ca^{2+} + Na_2C_2O_4 \rightarrow 2Na^+ + CaC_2O_4$

1 mole Ca^{2+} yields 1 mole CaC_2O_4

$1 \text{ ml EDTA} = 0.398 \text{ mg } Ca^{2+}$

$\text{chemical yield} = \frac{\text{actual weight}}{\text{predicted weight}} \times 100$

chemical yield for ^{49}Ti target from EDTA titration $= \frac{(0.398 \text{ mg/ml})(11.70 \text{ ml})(100)}{(5.06 \text{ mg})}$

$= 92.1\%$

Calibration of Beta Counter

^{45}Ca disintegration rate = 4.85×10^5/min.

$$\varepsilon = \frac{^{45}Ca \text{ activity}}{^{45}Ca \text{ disintegration rate}}$$

Samples	1	2	3	4	5	6	7
mg/cm^2	2.13	4.42	6.96	8.11	10.3	12.2	14.5
A, counts/min.	17,882	13,531	17,198	14,416	12,689	11,416	11,339
chemical yield, %	53.1	62.0	99.1	88.0	94.9	84.4	97.4
ε, %	5.79	4.50	3.54	3.34	2.76	2.83	2.38

for ^{49}Ti (7.94 mg/cm^2) from plot, ε = 3.33%

Calibration of Gamma Counter

$$N_o = 6.73 \times 10^4/\text{sec.}$$

$$A_o = 511/\text{sec.}$$

$$\varepsilon = \frac{511/\text{sec.}}{6.73 \times 10^4/\text{sec.}}$$

$$\varepsilon = 7.59 \times 10^{-3}$$

Monitor Calculations

front monitor = 0.0175 g

rear monitor = 0.0176 g

average weight of monitor = 0.0175 g

From computer analysis,

front monitor, A_o = 732 counts/min.

rear monitor, A_o = 738 counts/min.

Activity in rear monitor slightly larger due to scattering of beam, and an average activity was taken.

average A_o = 735 counts/min.

from reference (1), σ for $^{27}Al(p, 3p3n)^{22}Na$ at 350 MeV = 14.8 mb

$$N_o = \frac{A_o}{(ce)\lambda}$$

$$= \frac{735 \text{ counts/min.}}{(7.59 \times 10^{-3})(5.07 \times 10^{-7}/\text{min.})}$$

$$= 1.92 \times 10^{11} \text{ atoms of } ^{22}Na \text{ at the end of the irradiation}$$

Target Calculations

From computer analysis,

$$A_o = 151.5 \text{ counts/min.}$$

$$N_o = \frac{A_o}{(ce)(cy)\lambda}$$

assuming no decay during irradiation where

ce = counting efficiency

cy = chemical yield

$\lambda = 2.92 \times 10^{-6}$/min.

$$N_o = \frac{151.5 \text{ counts/min.}}{(0.0333)(0,921)(2.92 \times 10^{-6}/\text{min.})}$$

$$N_o = 1.69 \times 10^9$$

Cross section, σ, for ^{45}Ca from ^{49}Ti,

$$\sigma = \sigma(\text{monitor}) \frac{(N_o \text{ of } ^{45}Ca)}{(N_o \text{ of } ^{22}Na)} \times \frac{(\text{at. wt. Ti})}{(\text{at. wt. Al})} \times \frac{(\text{wt. Al})}{(\text{wt. Ti})}$$

For ^{49}Ti,

$$\sigma = \frac{(14.8 \text{ mb})(1.69 \times 10^9)(49)(17.5 \text{ mg})}{(1.92 \times 10^{11})(27)(0.610 \text{ mg})}$$

$$\sigma = 6.80 \text{ mb}$$

Each cross section must be corrected for enrichment content

$$= \frac{6.80 \text{ mb}}{.7614}$$

$$= 8.93 \text{ mb}$$

Subtracting the 18.54% contribution of ^{48}Ti to the ^{49}Ti cross section,

average σ for ^{48}Ti at 350 MeV = 4.07 mb

for ^{49}Ti = 8.93 mb - (.1854)(4.07 mb)

= 8.17 mb

σ values were averaged for each isotope, and $\pm$ 13% limits calculated for the means.

Appendix B

TABLE 4

Tabulation of Data

Determination	1	2	3	4	5	6
			^{47}Ti			
Monitors						
A_o, counts/min	496.0	1,128.0	1,694.0	970.0	683.0	
σ, mb	14.8	14.8	14.8	14.8	14.8	
N ($\times 10^{11}$)	1.30	2.95	4.43	2.56	1.80	
Targets						
mg/cm^2	1.12	0.782	0.782	0.760	0.760	
mg Ti	1.01	0.751	0.751	0.727	0.727	
Yield, %	91.3	88.1	75.5	80.1	47.9	
Efficiency, %	2.94	3.15	3.48	3.22	4.07	
A_o, counts/min	47.5	94.6	112.5	56.7	35.9	

TABLE 4 (Continued)

Determination	1	2	3	4	5	6
N (x 10^8)	6.06	11.7	14.7	7.53	6.31	
σ, mb	2.08	2.39	2.00	1.85	2.20	
Corrected σ, mb	2.62	3.01	2.52	2.33	2.77	
Adjusted σ, mb	1.94	2.33	1.84	1.65	1.76	
			^{48}Ti			
Monitors						
A_o, counts/min	1,694.0	677.0	842.0	970.0	683.0	
σ, mb	14.8	14.8	14.8	14.8	14.8	
N (x 10^{11})	4.43	1.77	2.22	2.56	1.80	
Targets						
mg/cm^2	1.05	0.673	0.673	0.665	0.665	

TABLE 4 (Continued)

Determination	1	2	3	4	5	6
mg Ti	1.01	0.648	0.648	0.642	0.642	
Yield, %	89.7	48.9	97.4	73.8	91.6	
Efficiency, %	3.15	4.15	2.85	3.45	3.43	
A_o, counts/min	323.2	57.6	119.3	99.5	91.8	
N ($\times 10^9$)	3.92	9.72	1.47	1.34	1.00	
σ, mb	4.06	3.99	4.71	3.71	4.03	
Corrected σ, mb	4.10	4.03	4.75	3.74	4.06	
			^{49}Ti			
Monitors						
A_o, counts/min	735.0	1,128.0	677.0	842.0	970.0	683.0

TABLE 4 (Continued)

Determination	1	2	3	4	5	6
σ, mb	14.8	14.8	14.8	14.8	14.8	14.8
N (x 10^{11})	1.92	2.95	1.77	2.22	2.56	1.80
Targets						
mg/cm^2	0.630	0.630	0.620	0.620	0.808	0.808
mg Ti	0.610	0.610	0.602	0.602	0.785	0.785
Yield, %	92.1	85.4	88.7	98.2	78.4	27.0
Efficiency, %	3.33	3.50	3.16	2.65	3.60	4.95
A_o, counts/min	151.5	198.2	154.2	186.5	249.2	75.0
N (x 10^9)	1.69	2.27	1.88	2.45	3.02	1.92
σ, mb	6.80	5.96	8.48	8.62	7.06	6.46
Corrected σ, mb	8.93	7.83	11.1	11.3	9.21	8.48
Adjusted σ, mb	8.16	7.06	10.3	10.5	8.44	7.71

TABLE 4 (Continued)

Determination	1	2	3	4	5	6
			^{50}Ti			
Monitors						
A_o, counts/min	1,694.0	677.0	842.0	970.0	683.0	
σ, mb	14.8	14.8	14.8	14.8	14.8	
N (x 10^{11})	4.43	1.77	2.22	2.56	1.80	
Targets						
mg/cm^2	1.22	1.07	1.07	0.836	0.836	
mg Ti	1.19	1.04	1.04	0.819	0.819	
Yield, %	90.5	74.3	81.6	65.7	74.6	
Efficiency, %	3.53	3.17	3.23	3.66	3.26	
A_o, counts/min	778.2	206.1	328.7	205.9	169.0	
N (x 10^9)	8.35	3.00	4.27	2.93	2.38	

TABLE 4 (Continued)

Determination	1	2	3	4	5	6
σ, mb	7.64	7.99	8.87	6.82	7.83	
Corrected σ, mb	10.0	10.5	11.6	8.93	10.2	
Adjusted σ, mb	9.26	9.76	10.9	8.19	9.46	

APPENDIX C

STEPS TAKEN DURING MONTE CARLO CASCADE CALCULATIONS FROM REFERENCE 13

1. The projectile is followed across the nuclear surface and decides, inside the nucleus, where the first interaction takes place.

2. The kind and momentum of the struck particles is next determined.

3. The type of interaction, either elastic or inelastic, is determined.

4. The angles and energies of the reaction products are determined.

5. The calculation follows all nucleons struck during the cascade until they either leave the nucleus or are recaptured.

6. Each nucleon-nucleon collision is characterized by its own probability distribution for occurance, energy, and angular distribution of the collision partners.

7. A random choice is made at every point in the calculation where a decision is to be made.

8. If each random choice is weighted according to the probability distribution for the event in question, and if many events are calculated, the result should be characteristic of the overall process.

VITA

Dennis Paul Swauger

Born in Wilkinsburg, Pennsylvania, November 7, 1951. Graduated from Bridgeport Senior High School, Bridgeport, West Virginia, in June 1969. B.S. University of Pittsburgh, August 1973. Entered College of William and Mary, September 1973, as a full time student concentrating in chemistry. With the course requirements completed, became an M.A. candidate, May 1975.